Review of Scientific Instruments

The Macquarie Deformation-DIA facility at the Australian Synchrotron: A tool for high-pressure, high-temperature experiments with synchrotron radiation

Cite as: Rev. Sci. Instrum. **91**, 114501 (2020); https://doi.org/10.1063/5.0022849
Submitted: 26 July 2020 . Accepted: 26 October 2020 . Published Online: 12 November 2020

Nicholas Farmer, Tracy Rushmer, Jeremy Wykes, and Guilherme Mallmann

Review of Scientific Instruments ARTICLE scitation.org/journal/rsi

The Macquarie Deformation-DIA facility at the Australian Synchrotron: A tool for high-pressure, high-temperature experiments with synchrotron radiation

Cite as: Rev. Sci. Instrum. 91, 114501 (2020); doi: 10.1063/5.0022849
Submitted: 26 July 2020 • Accepted: 26 October 2020 •
Published Online: 12 November 2020

Nicholas Farmer,[1,a)] Tracy Rushmer,[1] Jeremy Wykes,[2] and Guilherme Mallmann[3]

AFFILIATIONS

[1]Department of Earth and Environmental Sciences, Macquarie University, Macquarie Park, NSW 2109, Australia
[2]Australian Synchrotron, 800 Blackburn Road, Clayton, VIC 3168, Australia
[3]Research School of Earth Sciences, Australian National University, Acton, ACT 2601, Australia

[a)]**Author to whom correspondence should be addressed:** nick.farmer@mq.edu.au

ABSTRACT

The Macquarie University Deformation-DIA (MQ D-DIA) multi-anvil apparatus at the Australian Synchrotron provides a new experimental facility that enables simultaneous high-pressure and high-temperature *in situ* synchrotron experimentation in Australia. The MQ D-DIA can be easily deployed at any of a number of beamlines at the Australian Synchrotron, and we describe its installation at the x-ray absorption spectroscopy beamline, which enables *in situ* x-ray absorption near-edge spectroscopy and energy-scanning x-ray diffraction. A simple, reliable, and x-ray transparent high-pressure cell assembly has been developed for the D-DIA for which load/pressure and heater power/temperature relationships have been calibrated using *in situ* x-ray diffraction and "offline" mineral equilibration experiments. Additionally, we have mapped temperature distribution within the assembly using a new quantitative electron microprobe mapping technique developed for fine-grained polyphase samples. We are now investigating the speciation of geologically important trace elements in silicate melts (e.g., Zr, U, and Th) measured *in situ* under high pressure and temperature conditions corresponding to the Earth's mantle. Pressure-dependent changes in speciation influence partitioning behavior, and therefore the distribution in the Earth, of many trace elements. However, previous *ex situ* investigations are hampered by uncertainty as to whether high-pressure speciation can be faithfully recorded in samples recovered to ambient conditions. We present preliminary results showing an increase in the coordination number of Zr dissolved as a trace component of a sodium-rich silicate melt with pressure. These results also indicate that silicate melt composition exerts a strong influence on Zr speciation.

INTRODUCTION

Most of the Earth's interior is inaccessible by direct or indirect sampling, compelling geoscientists to use laboratory experiments to recreate the high pressure–temperature conditions in the deep Earth. There is a complementary relationship between the fields of high-pressure experimental mineral physics, in which mineral pressure–volume–temperature (PVT) properties, stress–strain relationships, and partial melting of multi-phase rocks are investigated, and deep-Earth geophysics, in which properties such as seismic velocities, anisotropies, and density at depth are inverted from seismic data. However, quantitative experimental studies of minerals and melts under deep mantle conditions are challenging, and significant progress in this area has been associated with the development of new techniques. By combining new developments in high-pressure apparatus and synchrotron-based *in situ* measurements, a new generation of experimental studies of minerals and melts under deep-mantle conditions is emerging.

The Macquarie University Deformation-DIA (MQ D-DIA) apparatus at the Australian Synchrotron provides the Australian

Earth Science community with a facility for *in situ* synchrotron high pressure–temperature experimentation under conditions of the Earth's upper mantle, conditions encompassing the source of almost all magmas, and the major rheological and thermal transitions that govern the character of plate tectonics.

MOTIVATION

The partitioning of elements between silicate melts and minerals determines the distribution of elements in the Earth's crust and mantle. The speciation (valence state and coordination environment) of elements in silicate liquids becomes an increasingly important control on this partitioning behavior with pressure,[1] and there is abundant evidence from quenched and annealed glasses that the coordination numbers of many cations in silicate melts begin to change at pressures as low as ~3 GPa.[2,3] This implies that partitioning behavior observed at ambient or low pressure cannot necessarily be extrapolated to the conditions of the Earth's mantle. However, the extent to which these changes in speciation are preserved in glasses recovered from high pressure, high temperature conditions for conventional *ex situ* analysis is unclear even when annealing techniques are used, as quench rates are in the order of 650 °C/s in conventional multi-anvil apparatus and far slower in piston-cylinder apparatus.[4]

Using the MQ D-DIA, measurements employing synchrotron radiation can be made of large samples (up to ~5 mm^3) under pressure and temperature conditions up to ~6 GPa and ~1500 °C, respectively, simulating the upper mantle to a depth of up to ~150 km. DIA- or Osugi-type apparatus has a long history of use at synchrotron light sources.[5–7] To date, we have the MQ D-DIA to conduct *in situ* x-ray diffraction and to record the *in situ* x-ray absorption near edge structure (XANES) spectra of geologically important trace elements such as Zr in silicate liquids with simplified compositions.

X-RAY SOURCE AND CONTEXT WITHIN THE AUSTRALIAN SYNCHROTRON

The x-ray absorption spectroscopy (XAS) beamline at the 3 GeV Australian Synchrotron comprises a 1.9 T, multipole wiggler source (20 period), a vertical collimating mirror (Pt, Rh, and Si stripes), cryogenically cooled fixed-exit double crystal monochromator (DCM) with Si 111 and Si 311 crystals, and a toroidal refocusing mirror (Pt and Rh stripes).[8] Energies of ~4 keV–34 keV are accessible using the collimating and refocusing mirrors, permitting harmonic rejection to $<10^{-5}$; energies up to ~54 keV are accessible in "mirrorless" mode, with a greater harmonic content.

The beamline possesses two experimental hutches in addition to the optical enclosure. The first hutch, "hutch B," is dedicated to conventional XAS experiments and XAS experiments employing small *in situ* apparatus. The second experimental hutch, "hutch C," is completely reconfigurable and accommodates the MQ D-DIA press (Fig. 1).

A focused beam size of ~250 μm is possible at the sample location in hutch C. Flux at the focal spot is in the order of 10^{12} photons/s. The bright wiggler source, refocusing optics, and low harmonic content make the XAS beamline well suited to demanding, flux-limited applications such as high pressure–temperature *in situ* investigations.

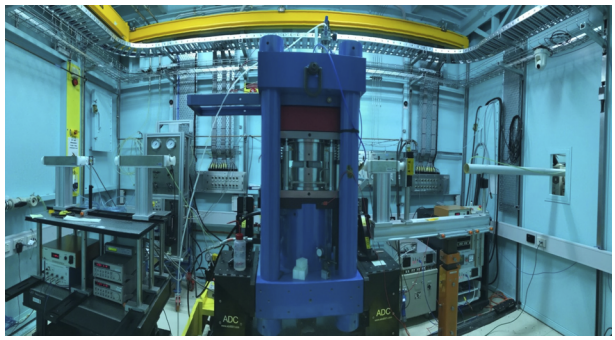

FIG. 1. View of the MQ D-DIA apparatus, a setup for *in situ* XAS in hutch C of the XAS beamline, similar to the setup shown in Fig. 7. The beam passes from right to left, entering the hutch through the tube.

THE D-DIA PRESS

The MQ D-DIA is a Deformation-DIA-type multi-anvil press in which six anvils act on a solid assembly, which can be either cubic or cuboidal. It is a development of the DIA- or Osugi-type cubic anvil apparatus[5,6,9,10] with the addition of two differential rams capable of driving the top and bottom anvils independently of the four horizontal anvils in order to impose deviatoric stress on a sample.[11] The MQ D-DIA apparatus can be operated as a standard cubic anvil apparatus without the differential rams to produce a near-hydrostatic high-pressure sample environment.

In hydrostatic mode, all six anvils are driven by a single hydraulic ram, which acts on the lower of two identical guide blocks, while the upper guide block is fixed. The upper and lower anvils are driven directly by the guide blocks, while the four horizontal anvils are advanced by wedge-shaped thrust blocks. The anvils are tungsten carbide with square truncations. When appropriately set up with shims, there is a cubic volume between the anvils. The anvils are interchangeable, and so far, we have used anvils with 4 mm edge-length truncations (Figs. 2 and 3).

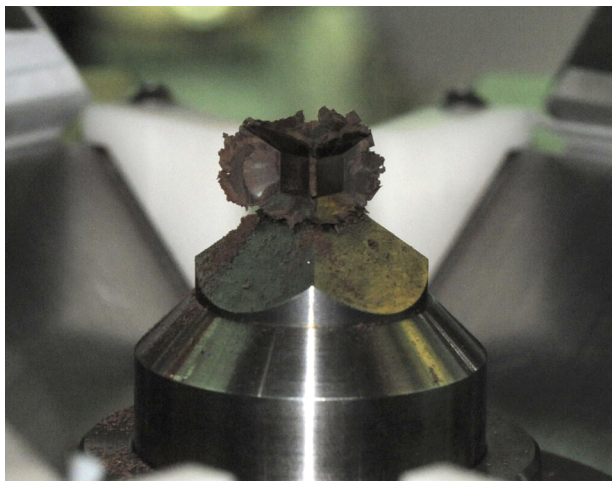

FIG. 2. 7 mm boron–epoxy assembly resting on the lower anvil after an experiment. Note: gaskets formed by extrusion of boron–epoxy from the assembly.

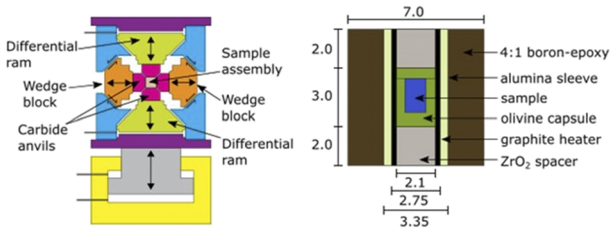

FIG. 3. Sketch of the D-DIA wedge block and anvil geometry (left); sketch of the 7 mm DIA assembly with the olivine capsule.

Hydraulic system

The main ram is driven by a hydraulic system comprising an Enerpac 0.5 hp submerged motor pump for coarse movement, a hand pump for fine manual control and establishing initial contact between the anvils and the pressure medium, and a stepper motor-driven syringe pump for automated high-pressure operation up to the load limit of 283 US tons. Pressure in the hydraulic system is monitored using a transducer and an 18-bit analog-to-digital converter (ADC). The motor driving the syringe pump is computer-controlled and can increase, decrease, and maintain the press load using a proportional–integral–derivative (PID) control loop implemented in the Experimental Physics and Industrial Control System (EPICS) used at the Australian Synchrotron. Diagrams showing the configuration of the hydraulic system and the motion control system through which it is operated can be found in the supplementary material (Figs. S7 and S8). During long experiments, this system is able to automatically maintain the press load within 0.2 US tons, which corresponds to <0.05 GPa sample pressure using the 7 mm assembly detailed below.

Heating system

The heating system comprises a Eurotherm 3504 process controller that outputs an analog voltage to a Eurotherm EFit phase angle silicon-controlled rectifier (SCR) that drives a multitap step-down transformer. The taps on the primary winding are at 80%, 100%, and 120% giving 6.25 V, 5.00 V, and 4.20 V, 200 A output, and are manually selectable by a switch. The Eurotherm process controller is equipped with five analog inputs, configured as two thermocouple inputs, voltage and current measured on the secondary side of the transformer, and the main ram pressure transducer. Thus, the heater can be controlled with either thermocouple or calculated power as the input to the PID loop; PID calculations are conducted by the EPICS control system. A diagram of the heating system is presented in the supplementary material (Fig. S9).

Positioning system

The press is positioned via a motion system based on the design in use at GSECARS (13-BM-D, APS) that provides movement along three perpendicular axes (x, y, z) and rotation about the vertical axis (Ω), which are controlled through EPICS via a Delta Tau Geobrick-LV motion controller.

The apparatus is mounted on large castors and all additional hardware such as the transformer and heater control system and pressure generator are portable, so the apparatus can be easily moved around the Australian Synchrotron facility. Not only can the MQ D-DIA be installed at any beamline with space to accommodate it, but experiments can also be conducted offline without any disruption to beamline schedules. This is particularly useful for offline calibration, assembly development, validation, and development of experimental techniques.

Assembly

A high-pressure assembly employing a boron–epoxy pressure medium has been developed, which balances x-ray transparency, large sample volume, ease of construction, and reproducibility of sample conditions. Using an assembly with 7 mm edge length and anvils with 4 mm truncations, the maximum pressure attainable at the limit of the press load is expected to be >15 GPa, while the silicate melts that are the subject if our current investigations occur in the Earth at significantly lower pressure. While we would have been able to achieve the pressure conditions required using a larger assembly, the 7 mm assembly was chosen because it is small enough that a sufficient x-ray flux can be transmitted through the assembly and large enough that samples can be contained within mineral capsules, which is an important consideration for maintaining an environment in chemical equilibrium with regard to fO_2 and $aSiO_2$.

The assembly comprises a boron–epoxy cube (4:1 weight ratio of amorphous boron to Epotek 353ND epoxy), pressed with a cylindrical hole in the center using a carbide die with tool steel punches and a precision ground core rod. A suite of core rods with diameters at 50 μm increments permits matching of the hole in the cube with a particular batch of internal assembly parts to achieve a good fit. The pressed boron–epoxy cubes are cured at >80 °C for at least 12 h in a drying oven.

Through careful control of the mass of material pressed in the die, pressed cubes are ready for use without additional machining. It was found that the drilling of equatorial holes for thermocouples resulted in excessive deformation in the vicinity of the thermocouple at high pressure. Frequent failures of thermocouples prompted development of a new punch such that cubes can be pressed in two halves with an integrated equatorial thermocouple channel formed during pressing. Such development is ongoing. In the meantime, power-based heating control has been adopted as the standard procedure.

The central section of the assembly is formed from a cylindrical alumina insulator, with a cylindrical graphite heater (Figs. 3 and 4). Inside the heater, the sample is placed in the central 3 mm, with 2 mm zirconia plugs above and below. Inner assembly parts are fabricated by COMPRES.[12] When compressed, part of the boron–epoxy cube extrudes between the anvils, forming gaskets.

Olivine capsules

An important distinction between this apparatus and those previously used to make XAS measurements at high pressure and temperature[13–19] is the provision of mineral capsules that allow for the buffering of chemical properties such as fO_2 and $aSiO_2$ that are critically important to the study of geological materials under

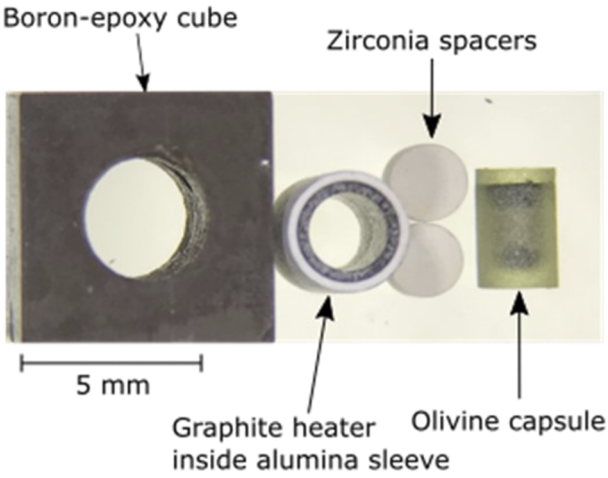

FIG. 4. Components of the MQ D-DIA assembly prior to assembly. In this example, the olivine capsule is made from naturally occurring olivine (San Carlos, AZ, USA).

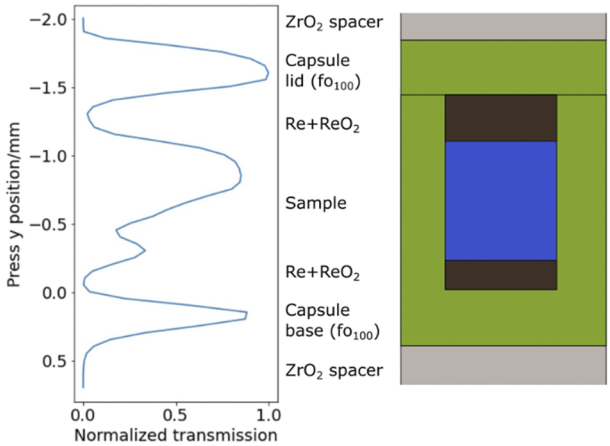

FIG. 5. X-ray transmission at 18 keV through the 7 mm D-DIA assembly under high pressure, high temperature conditions, recorded while translating the press vertically (y scan), showing greatest transmission through the lid and base of the synthetic forsterite capsule, and lower transmission through Re + ReO_2 powder than through the sample, here a sodic silicate liquid (NS2-fo).

high pressure and temperature conditions. In our XAS experiments, silicate melt samples were contained within olivine capsules and melt compositions were chosen to be close to, or in equilibrium with the capsule. Where redox-sensitive elements are investigated (e.g., U and Th), attempts to control fO_2 were made via the addition of Re–ReO_2 or Ru–RuO_2[20] as layers above and below the silicate liquid sample (Fig. 5).

MEASUREMENTS

XAS measurements

Transmission x-ray absorption spectroscopy measurements have been performed at high temperature and pressure using the

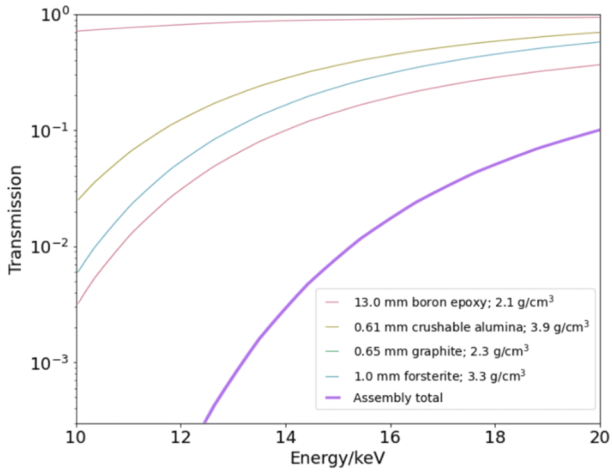

FIG. 6. Transmission through the sample assembly and olivine capsule, assuming 13 mm total length of boron–epoxy after extrusion of gaskets.

MQ D-DIA apparatus, with x-ray intensity measured up- and downstream of the press using ion chambers. When x-ray absorption measurements were collected, the position of the center of the sample was found by translating the press in the two axes perpendicular to the direction of the beam (x and y, Fig. 5). The toroidal refocussing mirror was used to focus the beam a size of <250 μm (horizontal and vertical), with the focus located ~50 cm behind the press, such that the beam is always converging through the sample. The size of the incident beam was further controlled by a set of slits in front of the press to a size smaller than the sample, and the beam profile was quantified by using one of the horizontal anvils as a knife-edge, horizontally scanning it through the beam, and monitoring the flux in the downstream ion chamber.

X-ray absorption measurements can be made readily at energies above 13 keV, where transmission of the assembly and forsterite capsule is $>10^{-4}$, and with increasing difficulty at lower energies. Below 12 keV energy, transmission through the assembly and capsule is $<10^{-4}$; at 10.5 keV, transmission is $<10^{-6}$ (Fig. 6).

X-ray diffraction

X-ray diffraction is a recent addition to the MQ D-DIA press. Inspired by the approach of Filipponi *et al.*,[21] an energy-scanning x-ray diffraction (ESXRD) setup has been constructed (Fig. 7) using

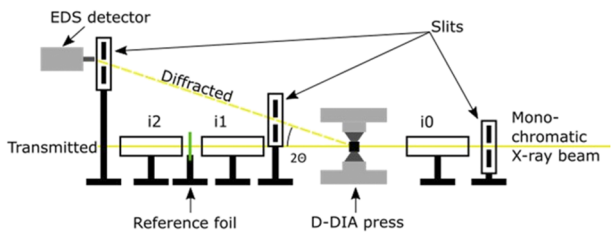

FIG. 7. Schematic diagram of the experimental setup for *in situ* XAS and XRD measurements in hutch C of the XAS beamline.

the x-ray absorption configuration with the addition of two sets of slits downstream of the press to collimate the diffracted beam and an x-ray detector (here, a single element vortex x-ray detector) from which the total incident x-ray intensity is measured. The detector and rearmost set of slits are directly above the downstream ion chambers, whereas the front slits are in front of the first downstream ion chamber and can be moved in and out of the beam path using a motorized stage, to permit x-ray absorption measurements. The detector and two sets of slits are aligned with the sample position at a fixed angle, using fluorescence from a ZrO_2 sample: ZrO_2 was mixed with cellulose and placed in the cavity of a 7 mm cellulose cube pressed using the same die used to produce boron–epoxy cubes. The alignment was conducted with the anvils in position, but not under load.

In this fixed-angle configuration, diffraction measurements are made by scanning the energy of the incident x rays using the DCM installed in the optics hutch at the XAS beamline, with an x-ray detector used to measure the intensity of diffracted x rays through the range of incident energies (Fig. 7). The energy scanning method possesses high incident energy resolution but with only a single x-ray detector and slit pair in our configuration, diffraction peaks cannot be measured in parallel, and the energy range is limited by the high energy cutoff imposed by the stripe materials of the collimating and toroidal focusing mirrors. The 2Θ angle of the diffraction setup is calibrated by diffracting in the energy range of the highest-amplitude peak in the sample material, then calculating Θ through Bragg's law, and taking d for the peak of interest from the JCPDS database.

SAMPLE CONDITIONS

Developing calibrations of the press load and heater power to sample pressure and temperature is especially important for the MQ D-DIA press, as it may be used offline or in various contexts in which x-ray diffraction (XRD) may not be possible.

Load–pressure calibration

We conducted a calibration of the press load to sample pressure by *in situ* XRD of a NaCl pressure standard. A pellet of NaCl, Au, and hexagonal BN (5:1:5 by mass) was loaded into the central sample chamber of a 7 mm assembly. This assembly was loaded into the press, and the NaCl 200 and Au 111 peaks were located with no pressure applied in order to calibrate 2Θ. After applying an initial 10 US tons of load using the hand pump, the load was increased steadily to 80 US tons over a period of 4.5 h. Diffraction patterns of the NaCl 200 and Au 111 peaks, each of which were acquired over ~5 min, were automatically collected every 30 min during the pressurization stage of the experiment [Fig. 8(a)].

Peak positions were determined from these patterns by fitting the peaks with a Pseudovoigt model using the lmfit software package[22] from which *d* spacing, and therefore unit cell volume, was calculated [Fig. 8(b)]. Diffraction peaks were somewhat broad [e.g., Fig. 8(a)] because the slits downstream from the sample were kept relatively wide to increase the x-ray flux to the x-ray detector (see Fig. 7), which effectively increased the range of 2Θ. Because this broadening effect had no effect on peak positions, the standard deviation fit from peak profiles overestimates uncertainty in these data. A Markov chain Monte Carlo method[23,24] was used to determine the degree to which uncertainty was overestimated, converging on a solution of $\sigma_{true} = 0.45 \times \sigma_{peakprofile}$. These corrected uncertainties are propagated through equation of state calculations. Details of this method are presented in the supplementary material.

At 80 US tons load, the unit cell volume of NaCl was 86% of the ambient-pressure volume (V_0), whereas the unit cell volume of Au was 97% of V_0. Pressure was calculated from the unit cell volume of NaCl using the equation of state of Dorogokupets and Dewaele[25] in the Pytheos software package.[26] Pressure was found to increase linearly with the press load up to 80 US tons, with $P(\text{GPa}) = 0.0668 \times load(\text{US tons}) - 0.085$ [Fig. 8(c)]. This indicates lower pressure at the given load than similar-sized boron–epoxy DIA assemblies used at different laboratories.[27–29]

Power–temperature calibration

XRD calibration

After the ambient-temperature–pressure calibration, a high-temperature calibration was attempted at 80 US tons load using the volumes of NaCl and Au to cross-calibrate pressure and temperature.[30–32] With load automatically maintained at 80 US tons, power was applied to the heater in 25 W increments up to 125 W above which power the heater became unstable and the experiment was discontinued. Diffraction patterns of the NaCl 200 and Au 111 peaks were collected at each power increment, and pressure and temperature were calculated by simultaneously fitting pressure and temperature the equations of state of both NaCl and Au.

To provide the values of pressure and temperature with reasonable estimates of uncertainty, a Markov chain Monte Carlo (MCMC) method was used to sample the probability distribution of pressure and temperature conditions for each combination of measured Au and NaCl volumes. This was accomplished using the emcee Python library[23] to conduct MCMC calculations, with equation of state calculations conducted using the Pytheos library.[26] At each 25 W increment, 10^6 samples of the probability distribution were calculated from which the reported values of pressure and temperature with uncertainties corresponding to ±1σ are derived. Details of this method can be found in the supplementary material.

The MCMC analysis shows strong covariance between errors in pressure and temperature, which reflects the oblique intersection of NaCl and Au isochores in P, T space. Uncertainty in pressure and temperature is ± ~80 K and ± ~0.15 GPa, similar to uncertainties reported in studies that employed similar methods of determining pressure and temperature from the intersection of NaCl and Au or hexagonal BN isochores.[30,31]

The heater power–temperature relationship is approximately linear up to 600 °C, with a gradient of ~5 °C/W [Fig. 8(e)]. Furthermore, the fit values of pressure are all close to the ambient-temperature value throughout this temperature range [Fig. 8(f)], showing that the ambient-temperature–pressure calibration can be extrapolated to high temperature, so long as the same sequence of compressing at ambient temperature then heating at the constant load is followed. Extension of the calibration to higher temperature awaits further beamtime.

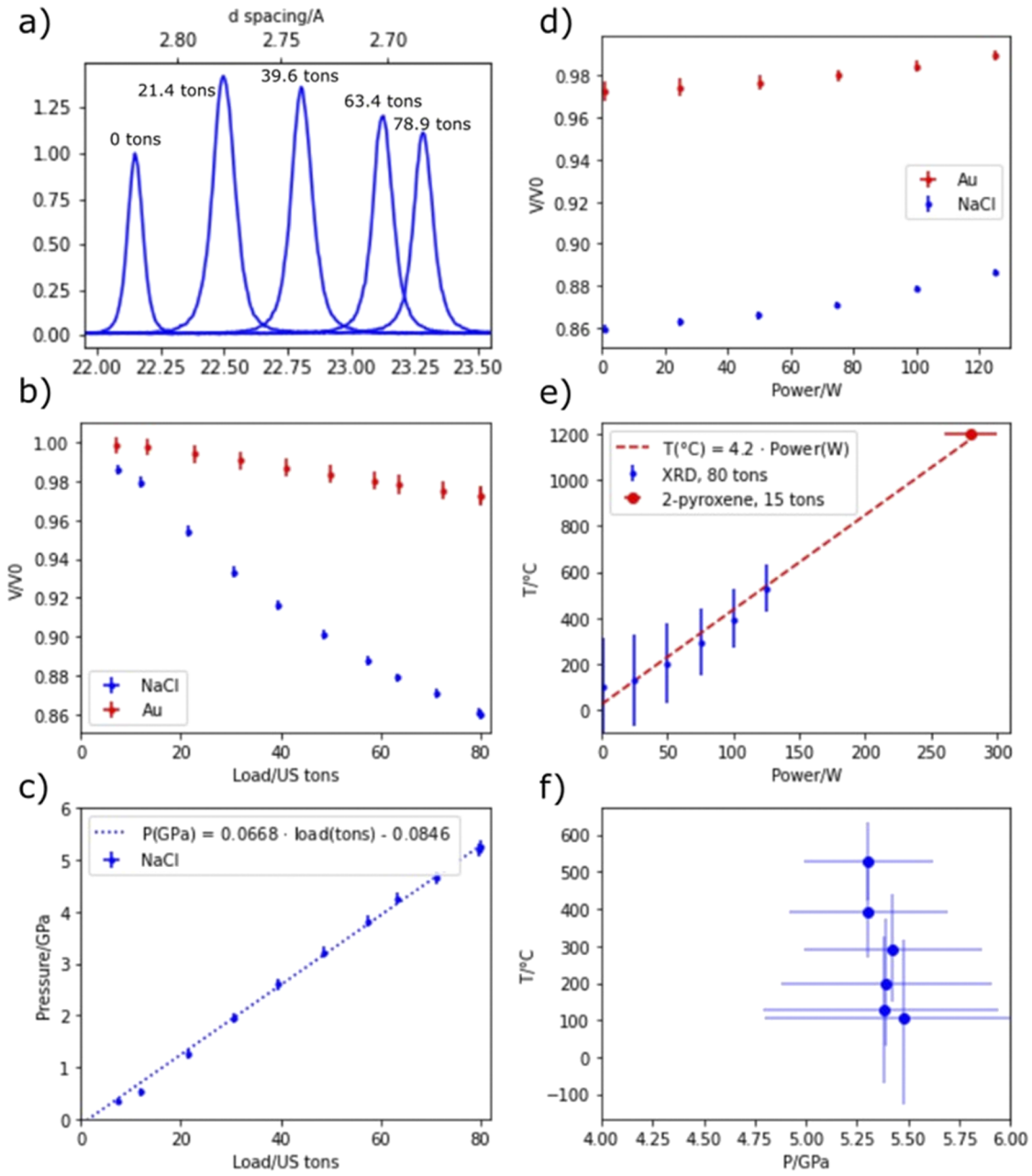

FIG. 8. Summary of XRD pressure calibration experiment. (a) NaCl 200 peak positions at different press loads; (b) calculated volume of NaCl and Au with the press load, error bars showing standard deviation determined using the Monte Carlo method; (c) ambient-temperature–pressure calibration from NaCl 200 equation of state,[25] error bars showing uncertainty in volume propagated through EoS; (d) NaCl and Au volume change with heating, error bars as in (d); (e) calculated temperature with heater power, error bars in XRD results indicate 1 standard deviation, determined using Markov chain Monte Carlo (MCMC) analysis (see the supplementary material); and (f) calculated pressure and temperature at the range of heater power, error bars as in (e).

Two-pyroxene thermometry and thermal gradients

In preparation for *in situ* experiments, offline experiments were conducted to measure temperature and thermal gradients within the cell through the equilibration of coexisting ortho- and clinopyroxene, a common method in determining the thermal properties of multi-anvil assemblies.[33–38] The starting material was a pellet of an oxide mix with a stoichiometry equivalent to 75 mol. % enstatite and 25 mol. % diopside. This was placed within a 7 mm assembly (Figs. 3 and 4) equipped with two equatorial

type-C thermocouples. The sample was pressurized to 15 US tons (0.92 GPa) and left for 72 hours with the constant output from the phase angle SCR. This experiment was conducted before the implementation of the PID power control system; in this case, heater power was controlled by setting the Eurotherm 3504 output to 34%, and heater power is estimated at 260 W–300 W from several subsequent experiments in which power was calculated from current and voltage measured on the secondary side of the transformer with the same constant Eurotherm output setting.

At the end of the experiment, the sample was quenched by turning off power to the heater and the sample recovered from the press. The entire assembly was cast in epoxy resin and sectioned vertically using a diamond saw. This section was polished, coated with 30 nm of carbon, and then analyzed using a JEOL 9300 electron probe microanalyzer at the Centre for Advanced Microscopy (ANU), with a 1 μm^2 beam, at 15 keV, 20 nA. Two modes of analysis were used, quantitative spot analyses of closely associated *ortho*- and *clino*-pyroxene were measured, calibrated against a diopside standard (Astimex Ltd., Toronto), and maps of Ca, Mg, and Si Kα intensity at 1 μm spacing through the entire central section of the assembly were collected (Fig. 9). Kα intensity maps and spot analyses were measured using thallium acid phthalate (TAP) crystals for Si and Mg and a pentaerythritol (PET) crystal for Ca.

A new approach to experimental thermometry is employed here: The Ca Kα intensity map is divided into 50 × 50 μm^2 bins, and the intensities through the entire bin are plotted as a histogram. The positions of the peaks of this histogram correspond to the composition of the orthopyroxene and clinopyroxene crystals within the bin. The peaks corresponding to each phase are fit for each 50 × 50 μm^2 bin, and then, these peak positions are compared to spot analyses at several points throughout the capsule to calculate a conversion factor from Ca Kα intensity to composition. In this way, the composition for ortho- and clinopyroxene is calculated for each 50 × 50 μm^2 bin; these data are then smoothed using a Gaussian function to remove noise, and the equation of Nickel *et al.*[39] is used to calculate the temperature at each position within the assembly. The resulting map shows measured temperatures throughout the sample, rather than an interpolation "by hand" between spot analyses as in previous work (Fig. 9).

This map and the accompanying profile through the center of the capsule (Fig. 9) show that the "hotspot" is offset toward the bottom of the sample volume; in the lower 1 mm of the mapped region, sample temperature varies by <100 °C; if thermal gradients are symmetrical and the hottest point is just above the bottom of this sample, then there is a region ~2 mm in length in which temperature varies by <100 °C, similar to the results of Wang *et al.*[11] using an assembly of similar size but different geometry.

The hottest part of the assembly measured is ~1200 °C, at the bottom of the sample. The flatness of the temperature profile in this region suggests that this is the hottest region of the assembly. This temperature is consistent with the power–temperature relationship measured by XRD up to 125 W [Fig. 8(e)] and suggests that the power–temperature relationship in this assembly does not vary drastically with sample pressure. However, this also demonstrates that deformation associated with equatorial thermocouple holes alters the position of the hot spot relative to the geometric center of the assembly, leading us to conclude that, given that

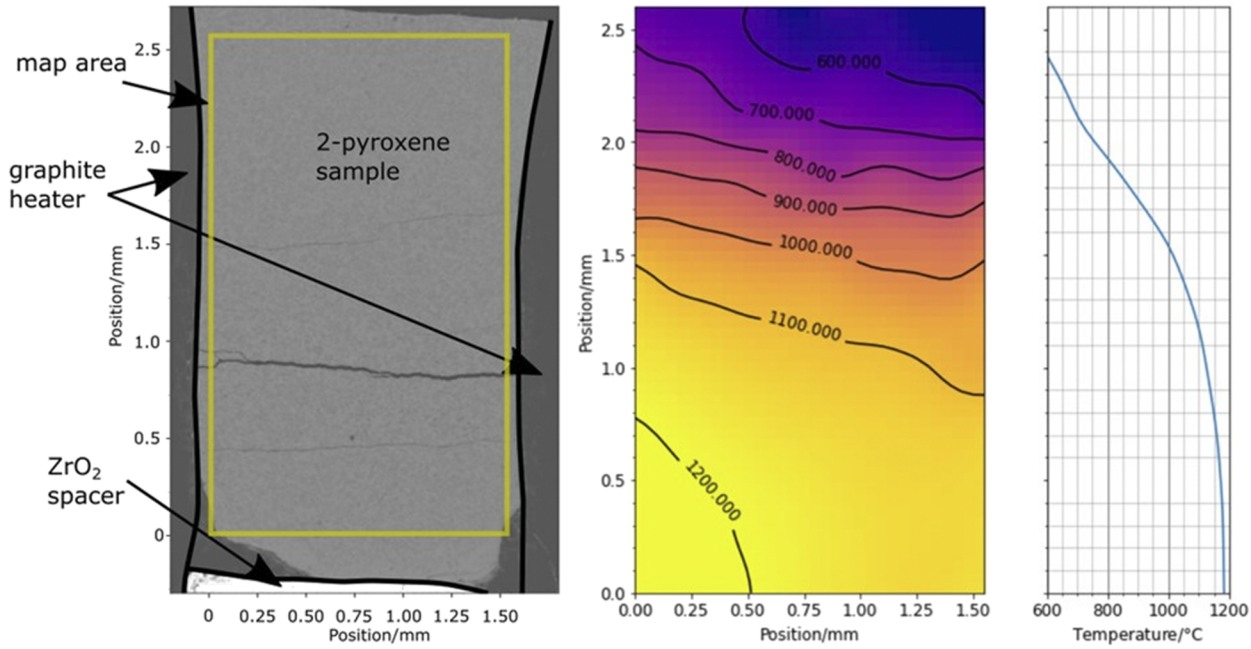

FIG. 9. Backscattered electron image and temperature map of the two-pyroxene experiment, with 100 °C gradients showing temperature variations through the sample and vertical temperature profile through the sample.

thermocouples in these experiments have a low success rate, heating based on calculated power is a more reliable and reproducible method.

XAS RESULTS

Preliminary *in situ* high-pressure, high-temperature x-ray absorption experiments have been conducted using the experimental setup depicted in Fig. 7.

Zr in silicate melt

XAS measurements were made *in situ* at high pressure and temperature of the Zr K-edge in a 75 wt. % $Na_2Si_2O_5$ 25 wt. % Mg_2SiO_4 (NS2-Fo) melt doped with 3 wt. % each of ZrO_2 and Nb_2O_5. Experiments were conducted using the standard assembly, with the silicate added as powder within the synthetic olivine (Fo_{100}) capsule, as well as Re and ReO_2 powders. In previous experiments, it was found that the buffer material was useful to contain the liquid within the capsule and to allow the sample position to be easily found during the experiment, so Re and ReO_2 powders were added despite the fact that the samples in these experiments are not redox sensitive. The sodic melt composition was chosen because of its far lower melting point compared to CMAS ($CaO–MgO–Al_2O_3–SiO_2$) compositions; partial melting and crystallization had been problematic in earlier experimental campaigns using higher melting point compositions.

Four experiments were conducted, at 20, 40, 60, and 80 US tons load (1.25 GPa, 2.56 GPa, 3.92 GPa, and 5.26 GPa), and measurements were made at 350 W heater power (~1470 °C), except in the 20 ton experiment, in which measurements were made at 325 W heater power (~1365 °C). Separate experiments were conducted at each pressure as the load/pressure calibration for multi-anvil apparatus is highly path-dependent, and no *in situ* pressure standard was used in these experiments. Each experiment was conducted using the same experimental routine of ambient-temperature compression, followed by heating while load is maintained automatically.

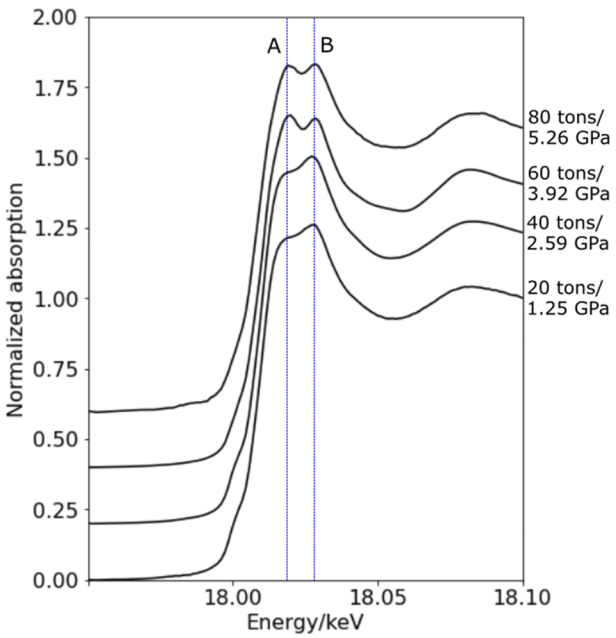

FIG. 10. K-edge x-ray absorption spectra of Zr showing variation with pressure.

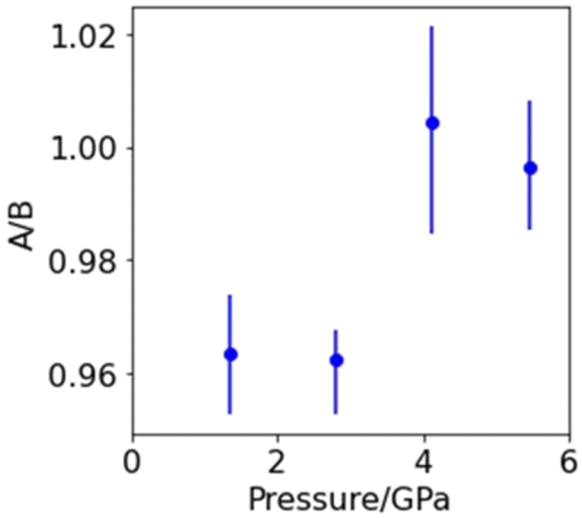

FIG. 11. Ratio of A to B peaks in Zr Ka with pressure. Error bars denote maximum and minimum values from measurements at each pressure.

These XAS measurements (Fig. 10) show a trend of the first peak of the white line (A) increasing in magnitude with pressure to the point of being of equal amplitude to the second peak (B). Wilke *et al.* linked the relative height of these peaks to Zr coordination, with "A" peaks of greater magnitude linked to Zr atoms with higher coordination numbers.[40] Measurements of Zr-bearing CMAS-7g (by weight: SiO_2 = 58.6%, Al_2O_3 = 12.3%, MgO = 2.4%, and CaO = 24.8%) glasses synthesized in the piston-cylinder and annealed close to the glass transition show a similar trend of increasing A/B with pressure, but with much greater change with pressure (A/B ~ 0.90–1.00 from 2 GPa to 6 GPa),[41] while these data (Fig. 11) show a change from ~0.96 to 1.00 in a similar pressure range (1.25 GPa–5.26 GPa).

This implies that while Zr coordination in CMAS and sodium silicate melts is similar at ~ 6 GPa, at lower pressure, Zr has a higher coordination in the sodium silicate melt than in the CMAS melt. This indicates that there is a strong compositional control on speciation of Zr in silicate melts, in addition to the effect of pressure.

CONCLUSION

The MQ D-DIA apparatus provides high pressure, high temperature capabilities at the Australian Synchrotron. Development work so far has established the calibration of sample pressure and temperature conditions to the press load and heater power, a vital precondition for use in offline applications or where the synchrotron

beamline does not allow XRD. We have demonstrated that high-quality *in situ* XANES analysis of silicate melts can be achieved using this apparatus, and we are working on applying this capability to trace elements important for geological processes.

SUPPLEMENTARY MATERIAL

The supplementary material includes diagrams of the hydraulic and motion control systems for pressure generation, a diagram of the heating and temperature control system used on the MQ-DDIA press, and a description of the Markov chain Monte Carlo method using the XRD pressure and temperature calibration, with further figures.

ACKNOWLEDGMENTS

We would like to thank Antony Burnham for discussions about the results of his study referenced herein. Our thanks are also due to everyone who has participated in D-DIA experiments at the AS, including Zsanett Pintér, Zachary Sudholz, Greg Yaxley, Laura Miller, Andrew Berry, Chris Cline III, Simon Clark, Simon Turner, and Alistair Hack. J.L.W. would like to thank the following for their assistance during the construction and commissioning of the MQ DDIA: William Rambold, Nader Afshar, Jai Cornes, Ben Baldwinson, and Andy Starritt from the AS Controls Group; Robert Grubb, Alan Easdon, Robert Rostan, Craig Hodgson, Trent Smith, and Jim Divitcos from the AS Engineering Group; David Cassar from Fort Minor Engineering; David Clark from RSES, ANU; Hans Mueller from GFZ; and Yanbin Wang, Julien Gasc, Feng Shi, Tony Yu, and Mark Rivers from GSECARS. We acknowledge the support from the Australian Research Council LIEF grant (Grant No. LE120100076) to Macquarie University, the Australian National University, and Monash University. We also acknowledge the facilities and the scientific and technical assistance of Microscopy Australia at the Advanced Imaging Precinct, Australian National University, a facility that is funded by the University, and State and Federal Governments, and in particular the assistance of Jeff Chen with EPMA analysis. N.F. acknowledges the support from a Ph.D. scholarship funded through Australian Research Council Grant No. FL130100066 awarded to Professor Hugh O'Neill. G.M. acknowledges support from the Australian Research Council (Grant No. DE160100169).

DATA AVAILABILITY

The data that support the findings of this study are available from the corresponding author upon reasonable request.

REFERENCES

[1]K. Mibe, M. Kanzaki, T. Kawamoto, K. N. Matsukage, Y. Fei, and S. Ono, J. Geophys. Res.: Solid Earth **112**, B03201, https://doi.org/10.1029/2005jb004125 (2007).
[2]Y. Wang, T. Sakamaki, L. B. Skinner, Z. Jing, T. Yu, Y. Kono, C. Park, G. Shen, M. L. Rivers, and S. R. Sutton, Nat. Commun. **5**, 3241 (2014).
[3]S. Bista, J. F. Stebbins, W. B. Hankins, and T. W. Sisson, Am. Mineral. **100**, 2298 (2015).
[4]D. Bondar, H. Fei, A. C. Withers, and T. Katsura, Rev. Sci. Instrum. **91**, 065105 (2020).
[5]O. Shimomura, S. Yamaoka, T. Yagi, M. Wakatsuki, K. Tsuji, H. Kawamura, N. Hamaya, O. Fukunaga, K. Aoki, and S. Akimoto, *Solid State Physics Under Pressure* (KTK Scientific Publishers, Tokyo and D. Reidel Publishing Company, Dordecht, 1985).
[6]D. J. Weidner, M. T. Vaughan, J. K. Yanbin Wang, K. Leinenweber, X. Liu, A. Yeganeh-Haeri, R. E. Pacalo, and Y. Zhao, High Pressure Res. **8**, 617 (1992).
[7]H. J. Mueller, F. R. Schilling, and C. Lathe, *Advances in High-Pressure Mineralogy* (Geological Society of America, 2007).
[8]C. Glover, J. McKinlay, M. Clift, B. Barg, J. Boldeman, M. Ridgway, G. Foran, R. Garret, P. Lay, and A. Broadbent, AIP Conf. Proc. **882**, 884–886 (2007).
[9]J. Osugi, K. Shimizu, K. Inoue, and K. Yasunami, Rev. Phys. Chem. Jpn. **34**, 1 (1964).
[10]S. Akimoto, T. Yagi, and K. Inoue, in *High-Pressure Research*, edited by M. H. Manghnani and S.-I. Akimoto (Academic Press, 1977), pp. 585–602.
[11]Y. Wang, W. B. Durham, I. C. Getting, and D. J. Weidner, Rev. Sci. Instrum. **74**, 3002 (2003).
[12]K. D. Leinenweber, J. A. Tyburczy, T. G. Sharp, E. Soignard, T. Diedrich, W. B. Petuskey, Y. Wang, and J. L. Mosenfelder, Am. Mineral. **97**, 353 (2012).
[13]O. Shimomura and T. Kawamura, in *High-Pressure Research in Mineral Physics*, edited by M. H. Manghnani and Y. Syono (1987), pp. 187–193.
[14]Y. Katayama, K. Tsuji, O. Shimomura, and H. Oyanagi, J. Non-Cryst. Solids **205-207**, 199 (1996).
[15]Y. Katayama, M. Mezouar, J. P. Itié, J. M. Besson, G. Syfosse, P. Le Fèvre, and A. Di Cicco, J. Phys. IV France **7**, C2 (1997).
[16]O. Ohtaka, H. Arima, H. Fukui, W. Utsumi, Y. Katayama, and A. Yoshiasa, Phys. Rev. Lett. **92**, 155506 (2004).
[17]F. Farges, S. Djanarthany, S. Wispelaere, M. Munoz, B. Magassouba, A. Haddi, M. Wilke, C. Schmidt, M. Borchert, P. Trocellier, W. Crichton, A. Simionovici, P. Petit, M. Mezouar, M.-P. Etcheverry, I. Pallot-Frossard, J. Bargar, G. Brown, Jr., D. Grolimund, and A. Scheidegger, Phys. Chem. Glasses: Eur. J. Glass Sci. Technol., Part B **46**, 350 (2005).
[18]B. Cochain, C. Sanloup, C. de Grouchy, C. Crépisson, H. Bureau, C. Leroy, I. Kantor, and T. Irifune, Chem. Geol. **404**, 18 (2015).
[19]J. Pohlenz, S. Pascarelli, O. Mathon, S. Belin, A. Shiryaev, O. Safonov, A. Veligzhanin, V. Murzin, T. Irifune, and M. Wilke, J. Phys.: Conf. Ser. **712**, 012083 (2016).
[20]M. I. Pownceby and H. S. C. O'Neill, Contrib. Mineral. Petrol. **118**, 130 (1994).
[21]A. Filipponi, V. M. Giordano, S. De Panfilis, A. Di Cicco, E. Principi, A. Trapananti, M. Borowski, and J.-P. Itiè, Rev. Sci. Instrum. **74**, 2654 (2003).
[22]M. Newville, T. Stensitzki, D. B. Allen, and A. Ingargiola (2014). "LMFIT: Non-linear least-square minimization and curve-fitting for Python," Zenodo. https://zenodo.org/record/11813.
[23]D. Foreman-Mackey, D. W. Hogg, D. Lang, and J. Goodman, Publ. Astron. Soc. Pac. **125**, 306 (2013).
[24]J. Goodman and J. Weare, Commun. Appl. Math. Comput. Sci. **5**, 65 (2010).
[25]P. I. Dorogokupets and A. Dewaele, High Pressure Res. **27**, 431 (2007).
[26]S.-H. D. Shim (2014). "Shdshim/pytheos: Before updating for Cider 2018," Zenodo. https://zenodo.org/record/802391.
[27]D. J. Weidner, M. T. Vaughan, J. Ko, Y. Wang, X. Liu, A. Yeganeh-Haeri, R. E. Pacalo, and Y. Zhao, *High-Pressure Research: Application to Earth and Planetary Sciences*, edited by Y. Syono and M. H. Manghnani (Terra Scientific Publishing Company, Tokyo, 1992), Vol. 67, p. 13.
[28]W. Utsumi, Rev. High Pressure Sci. Technol. **14**, 346 (2004).
[29]F. B. Hua, K.-C. Liang, J. Kung, W.-L. Hsu, and Y. Wang, Terr. Atmos. Ocean Sci. **23**, 647 (2012).
[30]T. Yagi, O. Shinomura, S. Yamaoka, K. Takemura, and S. Akimoto, *Solid State Physics Under Pressure: Recent Advances with Anvil Devices* (KTK Scientific Publishers, Tokyo, Japan, 1985), pp. 363–368.
[31]Y. Zhao, R. B. Von Dreele, D. J. Weidner, and D. Schiferl, High Pressure Res. **15**, 369 (1997).
[32]W. Crichton and M. Mezouar, High Temp. - High Pressures **34**, 235 (2002).
[33]E. Takahashi, H. Yamada, and E. Ito, Geophys. Res. Lett. **9**, 805, https://doi.org/10.1029/gl009i008p00805 (1982).

[34]T. Irifune and W. Hibberson, High Temp. - High Pressures **17**, 575 (1985).
[35]T. Gasparik, Contrib. Mineral. Petrol. **102**, 389 (1989).
[36]D. Canil, Contrib. Mineral. Petrol. **117**, 410 (1994).
[37]A. Shatskiy, I. S. Sharygin, P. N. Gavryushkin, K. D. Litasov, Y. M. Borzdov, A. V. Shcherbakova, Y. Higo, K.-i. Funakoshi, Y. N. Palyanov, and E. Ohtani, Am. Mineral. **98**, 1593 (2013).
[38]A. Zarei, Y. Li, H. Fei, and T. Katsura, High Pressure Res. **38**, 243 (2018).
[39]K. G. Nickel, G. P. Brey, and L. Kogarko, Contrib. Mineral. Petrol. **91**, 44 (1985).
[40]M. Wilke, C. Schmidt, J. Dubrail, K. Appel, M. Borchert, K. Kvashnina, and C. E. Manning, Earth Planet. Sci. Lett. **349-350**, 15 (2012).
[41]A. D. Burnham, C. Le Losq, H. St, C. O'Neill, and J. L. Wykes, *Goldschmidt Abstracts* (Geochemical Society, 2019), Vol. 436.